Letter | Editors' Suggestion

Analytic third-order QCD corrections to top-quark and semileptonic $b \to u$ decays

Long-Bin Chen,[1] Hai Tao Li,[2,*] Zhao Li,[3,4,5] Jian Wang,[2,5,†] Yefan Wang,[2,6,‡] and Quan-feng Wu[3,4]

[1]*School of Physics and Materials Science, Guangzhou University, Guangzhou 510006, China*
[2]*School of Physics, Shandong University, Jinan, Shandong 250100, China*
[3]*Institute of High Energy Physics, Chinese Academy of Sciences, Beijing 100049, China*
[4]*School of Physics Sciences, University of Chinese Academy of Sciences, Beijing 100049, China*
[5]*Center for High Energy Physics, Peking University, Beijing 100871, China*
[6]*Department of Physics and Institute of Theoretical Physics, Nanjing Normal University, Nanjing, Jiangsu 210023, China*

(Received 18 September 2023; accepted 7 March 2024; published 8 April 2024)

We present the first analytic results of next-to-next-to-next-to-leading-order (N^3LO) QCD corrections to the top-quark decay width. We focus on the dominant leading color contribution, which includes light-quark loops. At next-to-next-to-leading order (NNLO), this dominant contribution accounts for 95% of the total correction. By utilizing the optical theorem, the N^3LO corrections are related to the imaginary parts of the four-loop self-energy Feynman diagrams, which are calculated with differential equations. The results are expressed in terms of harmonic polylogarithms, enabling fast and accurate evaluation. The third-order QCD corrections decrease the leading-order decay width by 0.667%, and the scale uncertainty is reduced by half compared to the NNLO result. The most precise prediction for the top-quark width is now 1.321 GeV for $m_t = 172.69$ GeV. Additionally, we obtain the third-order QCD corrections to the dilepton invariant mass spectrum and decay width in the semileptonic $b \to u$ transition. The perturbative series in the on-shell mass scheme exhibits poor convergence behavior. In the $\overline{\text{MS}}$ mass scheme, the scale dependence is greatly improved. A more precise determination of the CKM matrix element V_{ub} could be obtained with such higher-order corrections.

DOI: 10.1103/PhysRevD.109.L071503

The top quark, which is the heaviest elementary particle, has been discovered for about twenty-eight years. Its mass has been measured to be $m_t = 174.41 \pm 0.39(\text{stat}) \pm 0.66(\text{syst}) \pm 0.25(\text{recoil})$ GeV [1], and its couplings with other particles have been probed with high precision. This provides necessary input parameters for the calculation of top-quark production processes—e.g., the top-quark pair productions at the hadron colliders. In realistic simulations of the top-quark events, the decay has to be taken into account as well, where the top-quark decay width, denoted by Γ_t, is indispensable. Moreover, the top-quark decay width would be modified in new physics models in which the top quark can decay to new particles. Therefore, a precise determination of the top-quark decay width can be used not only in the precise prediction of the top-quark production and decays, but also as a probe of new physics.

Generally, the top-quark decay width can be measured with direct and indirect approaches. The direct measurement exploits a profile likelihood fit of the observed data, such as the invariant mass of the lepton and b-jet, to the template distributions corresponding to different top-quark decay widths. The ATLAS Collaboration has performed a direct measurement using the top-quark pair events in the dileptonic channel at the 13 TeV LHC corresponding to an integrated luminosity of 139 fb^{-1}, obtaining a width of $\Gamma_t = 1.9 \pm 0.5$ GeV [2].

On the other hand, in indirect measurements, the decay width is extracted from quantities that depend on Γ_t. The CMS Collaboration has measured the branching ratio $B(t \to Wb)/B(t \to Wq)$ with $q = b, s, d$ using the $t\bar{t}$ events in the dileptonic channel at $\sqrt{s} = 8$ TeV. Combined with the measurement of the t-channel single top-quark cross section, the top-quark decay width is determined as $\Gamma_t = 1.36 \pm 0.02(\text{stat})^{+0.14}_{-0.11}(\text{syst})$ GeV [3]. Following the idea proposed to measure the Higgs boson's width [4], the top-quark width can also be derived by measuring both the on-shell and off-shell top-quark productions. The analyses for the single top

*Corresponding author: haitao.li@sdu.edu.cn
†Corresponding author: j.wang@sdu.edu.cn
‡Corresponding author: wangyefan@sdu.edu.cn

and top-quark pair productions show that an accuracy of 0.3 GeV can be reached [5–7].

The e^+e^- collider provides a good opportunity to determine the top-quark mass and width with high precision because the center-of-mass energy is tunable. The cross sections near the $t\bar{t}$ threshold are very sensitive to the top-quark mass and width. Assuming an integrated luminosity of 220 fb^{-1}, the determination of the top-quark width can be carried out with an accuracy at the 2% level [8–10].

To meet the requirements of both theory and experiment, much effort has been devoted to improving the predictions for top-quark decay. The next-to-leading-order (NLO) QCD corrections decrease the decay width by about 9% [11–13]. The next-to-next-to-leading-order (NNLO) QCD corrections provide a 2% suppression further [14–16]. The analytical form of the NNLO total width has been studied in the $w \equiv m_W^2/m_t^2 \to 0$ [17–20] and $w \to 1$ [21] limits, respectively. The NNLO polarized decay rates have been calculated in [22,23]. The dependence of the NNLO result on the renormalization scheme and scales was discussed in [24]. Recently, the three-loop color-planar master integrals [25] and form factors [26] of the heavy-to-light quark decays were obtained. The NLO electroweak (EW) corrections [27,28] and off-shell W-boson effects [11] have also been computed, and their contributions almost cancel each other.

The goal of this work is to provide the first analytic results of next-to-next-to-next-to-leading-order (N^{3}LO) QCD corrections. This is motivated by the fact that the NNLO corrections are beyond the scale-uncertainty band of the NLO corrections using the conventional scale variation—i.e., changing the renormalization scale by a factor of 2. It is interesting to see whether the N^{3}LO QCD corrections lie within the scale-uncertainty band of the NNLO corrections. Moreover, our analytic results present special data about the multiloop Feynman integrals and scattering amplitudes, since top-quark decay is the first physical process with massive colored particles that has been calculated at N^{3}LO analytically without any expansion of the loop integrals.

In the SM, the top quark decays via electroweak interaction to Wq with $q = b, s, d$ at leading order (LO), and the decay rate of $t \to Wq$ is proportional to the square of the Cabibbo-Kobayashi-Maskawa (CKM) matrix element V_{tq}. Since $V_{tb} \approx 0.999$ and $V_{ts}, V_{td} \leq 0.04$ [29], and the decay rates of $t \to Wq$ differ by a common factor, we consider only $t \to Wb$ in our calculation. Including higher-order QCD corrections, the top-quark width is written as a series of the strong coupling α_s,

$$\Gamma_t = \Gamma_0 \left[X_0 + \frac{\alpha_s}{\pi} X_1 + \left(\frac{\alpha_s}{\pi}\right)^2 X_2 + \left(\frac{\alpha_s}{\pi}\right)^3 X_3 \right], \quad (1)$$

with $\Gamma_0 = G_F m_t^3 |V_{tb}|^2/8\sqrt{2}\pi$. The first two coefficients, X_0 and X_1, have been calculated analytically thirty years ago [11–13]. The analytic form of the third coefficient, X_2, was obtained recently by four of the authors [16], and the result is given in different color structures by

$$\begin{aligned} X_2 &= C_F[C_F X_F + C_A X_A + T_R n_l X_l + T_R n_h X_h] \\ &= C_F \left[N_c \left(X_A + \frac{X_F}{2} \right) + \frac{n_l}{2} X_l - \frac{1}{2N_c} X_F + \frac{n_h}{2} X_h \right], \end{aligned} \quad (2)$$

where we have substituted in the bracket $C_F = (N_c^2 - 1)/2N_c$, $C_A = N_c$, and $T_R = 1/2$ in the second line and n_l (n_h) is the number of massless (massive) quark species. In our case, $N_c = 3$, $n_l = 5$, and $n_h = 1$, and thus we expect that the terms proportional to N_c or n_l, denoted as the *leading color* contribution, provide the dominant contributions. We find that the leading color contribution is significantly dominant, accounting for around 95% of the full NNLO correction for $w < 0.9$. Note that the NNLO correction is almost vanishing for $w > 0.9$, and that $w \approx 0.22$ in the top-quark decay.

As in Eq. (2), the result of X_3 is decomposed in color structures by

$$\begin{aligned} X_3 = C_F \Bigg[& N_c^2 Y_A + \tilde{Y}_A + \frac{\bar{Y}_A}{N_c^2} + n_l n_h Y_{lh} + n_l \left(N_c Y_l + \frac{\tilde{Y}_l}{N_c} \right) \\ & + n_l^2 Y_{l2} + n_h \left(N_c Y_h + \frac{\tilde{Y}_h}{N_c} \right) + n_h^2 Y_{h2} \Bigg]. \end{aligned} \quad (3)$$

We focus on the leading color coefficients Y_A, Y_l, and Y_{l2} that give the most dominant contributions. Our goal in this work is to present their analytic form.

In our method, the top-quark decay width Γ_t is related to the imaginary part of the amplitude of the process $t \to Wb \to t$ via the optical theorem,

$$\Gamma_t = \frac{\mathrm{Im}[\mathcal{M}(t \to Wb \to t)]}{m_t}. \quad (4)$$

In order to obtain the N^{3}LO QCD corrections, the calculation of four-loop self-energy Feynman diagrams is required.

We have used the FeAmGen program [30], which employs QGRAF [31] to generate four-loop Feynman diagrams and amplitudes. The amplitudes are manipulated with Form [32] and FeynCalc [33] to perform the Dirac algebra, and expressed as linear combinations of scalar loop integrals. Then, we utilize the FIRE6 package [34], which implements the LAPORTA algorithm [35] in solving the system of the integration-by-parts identities [36,37], to reduce all the scalar integrals into a set of master integrals (MIs). All the MIs belong to the integral family defined by

$$I_{n_1,n_2,\ldots,n_{14}} = \frac{1}{\pi} \mathrm{Im} \int \frac{\mathcal{D}^d k_1 \mathcal{D}^d k_2 \mathcal{D}^d k_3 \mathcal{D}^d k_4}{D_1^{n_1} D_2^{n_2} D_3^{n_3} \cdots D_{14}^{n_{14}}}, \quad (5)$$

with the propagators $D_1 = (k_1 + p)^2 - m_t^2$, $D_2 = (k_2 + p)^2 - m_t^2$, $D_3 = (k_3 + p)^2 - m_t^2$, $D_4 = (k_3 + k_4)^2$, $D_5 = (k_2 + k_4)^2$, $D_6 = (k_1 + k_4)^2$, $D_7 = k_1^2$, $D_8 = (k_1 - k_2)^2$, $D_9 = (k_2 - k_3)^2$, $D_{10} = (k_1 - k_3)^2$, $D_{11} = k_2^2$, $D_{12} = k_3^2$, $D_{13} = k_4^2$, $D_{14} = (k_4 - p)^2 - m_W^2$, and $\mathcal{D}^d k_i \equiv -i\pi^{-d/2} e^{-\epsilon\gamma} m_t^{2\epsilon} \mathrm{d}^d k_i$, $d = 4 - 2\epsilon$.

The external top quarks satisfy the on-shell condition $p^2 = m_t^2$. Notice that only the integrals with nonvanishing imaginary parts are relevant in our calculation. For the leading color contribution, we have about 40 000 scalar integrals, which are reduced to 185 MIs. These MIs involve two scales, m_W^2 and m_t^2, and therefore they can be expressed as functions of a single parameter w. Adopting the differential equation method [38–40], we remarkably succeed in constructing the canonical basis $\mathbf{B}$ of the MIs, which satisfies the differential equation

$$\frac{\mathrm{d}\mathbf{B}}{\mathrm{d}w} = \epsilon\left(\frac{\mathbf{P}}{w} + \frac{\mathbf{N}}{w-1}\right)\mathbf{B}, \tag{6}$$

with $\mathbf{P}$ and $\mathbf{N}$ being rational matrices. In some low sectors, the package Libra [41] has been used to transform coupled integrals to the canonical basis. In some high sectors, it is important to choose a basis integral with more propagators than the normal ones in the specified sector in order to achieve a compact form of the basis.

Solving the above equation recursively, we obtain analytical expressions for basis integrals in a series of ϵ with undetermined constants. For most of the integrals, these constants can be derived using the regularity conditions at $w = 0$ or $w = 1$. In practice, we also adopt another method. The coefficient of each order of ϵ has been written in terms of harmonic polylogarithms [42]. We evaluate these expressions in a fixed value of w within the region (0, 1)—e.g., $w = 1/4$, using the HPL package [43], and compare them with the high-precision numerical results by AMFlow [44,45] to determine the integration constants. Their analytic form is recovered by making use of the PSLQ algorithm [46,47]. The expressions of the master integrals are cross-checked with AMFlow at arbitrary values of w in $0 < w < 1$. Notice that the imaginary part of each four-loop self-energy diagram has only UV poles up to $1/\epsilon^3$, since all the IR divergences have canceled. These UV poles cancel out after including the contribution from counterterms. As a nontrivial test, the decay rate is finite and vanishing for $w = 1$ because no phase space exists.

The analytical results of Y_A, Y_l, and Y_{l2} in Eq. (3) are compact, and their complete forms and expansions around $w = 1$ have been provided in the Supplemental Material [48]. Here, we present the expansion series near the boundary $w = 0$:

$$\begin{aligned}
Y_A &= \left[\frac{203185}{41472} - \frac{12695\pi^2}{1944} - \frac{4525\zeta(3)}{576} - \frac{1109\pi^4}{25920} + \frac{37\pi^2\zeta(3)}{36} + \frac{1145\zeta(5)}{96} + \frac{47\pi^6}{2835} - \frac{3\zeta(3)^2}{4}\right] \\
&+ w\left[-\frac{157939}{2304} + \frac{140863\pi^2}{20736} + \frac{5073\zeta(3)}{64} - \frac{14743\pi^4}{6480} - \frac{169\pi^2\zeta(3)}{72} - \frac{45\zeta(5)}{16} + \frac{3953\pi^6}{22680} - \frac{15\zeta(3)^2}{4}\right] \\
&+ w^2\left[\log(w)\left(\frac{851099}{27648} - \frac{5875\pi^2}{2304} - \frac{33\zeta(3)}{8} + \frac{\pi^4}{10}\right) - \frac{82610233}{331776} + \frac{799511\pi^2}{27648}\right. \\
&\left. + \frac{4093\zeta(3)}{32} - \frac{5987\pi^4}{2880} - \frac{91\pi^2\zeta(3)}{16} - \frac{275\zeta(5)}{8} + \frac{347\pi^6}{3024} - \frac{9\zeta(3)^2}{8}\right] + \mathcal{O}(w^3), \\
Y_l &= \left[\frac{18209}{20736} + \frac{60025\pi^2}{31104} - \frac{197\zeta(3)}{288} - \frac{14\pi^4}{405} + \frac{5\pi^2\zeta(3)}{36} - \frac{25\zeta(5)}{12}\right] \\
&+ w\left[-\frac{179}{1152} - \frac{3709\pi^2}{2592} - \frac{73\zeta(3)}{6} + \frac{46\pi^4}{405} + \frac{19\pi^2\zeta(3)}{18} + \frac{5\zeta(5)}{2}\right] \\
&+ w^2\left[\log(w)\left(-\frac{11077}{1152} + \frac{37\pi^2}{96} + \frac{3\zeta(3)}{8}\right) + \frac{49097}{648} - \frac{817\pi^2}{128} - \frac{2651\zeta(3)}{96} + \frac{17\pi^4}{270} + \frac{5\pi^2\zeta(3)}{6} + \frac{25\zeta(5)}{4}\right] + \mathcal{O}(w^3), \\
Y_{l2} &= \left[-\frac{695}{2592} - \frac{91\pi^2}{972} + \frac{11\zeta(3)}{36} - \frac{2\pi^4}{405}\right] + w\left[\frac{245}{144} - \frac{73\pi^2}{648} - \frac{\zeta(3)}{3}\right] \\
&+ w^2\left[\log(w)\left(\frac{245}{432} - \frac{\pi^2}{72}\right) - \frac{791}{162} + \frac{85\pi^2}{432} + \frac{3\zeta(3)}{4} + \frac{2\pi^4}{135}\right] + \mathcal{O}(w^3),
\end{aligned} \tag{7}$$

where $\zeta(n)$ is the Riemann zeta function. We have set the renormalization scale $\mu = m_t$ in the above equations, and the full μ-dependent terms can be easily recovered from the running equation of the strong coupling. One can see that there is a single logarithm $\log(w)$ starting from $\mathcal{O}(w^2)$. This comes from the one-loop tadpole integral with a scale of m_W when expanding the four-loop integral in the small-w limit with the method of regions.

To see the impact of the N^{3}LO QCD corrections, we decompose the decay width according to the perturbative orders:

TABLE I. Top-quark width up to N^{3}LO and various higher-order corrections in percentage (%) with respect to the LO width $\Gamma_t^{(0)} = 1.486$ GeV. The values of $\delta_b^{(1)}$ and $\delta_{\rm EW}^{(1)}$ are calculated using the formulas in [11,27,49,50]. The notation "$*$" represents a correction that has not been calculated. The numbers in the last column show the decay width with all the available corrections up to that order. The scale uncertainties are also shown explicitly.

	$\delta_b^{(i)}$	$\delta_W^{(i)}$	$\delta_{\rm EW}^{(i)}$	$\delta_{\rm QCD}^{(i)}$	Γ_t [GeV]
LO	−0.273	−1.544	⋯	⋯	1.459
NLO	0.126	0.132	1.683	−8.575	$1.361^{+0.0091}_{-0.0130}$
NNLO	$*$	0.030	$*$	−2.070	$1.331^{+0.0055}_{-0.0051}$
N^{3}LO	$*$	0.009	$*$	−0.667	$1.321^{+0.0021}_{-0.0025}$

$$\begin{aligned}\Gamma_t = \Gamma_t^{(0)}[&(1+\delta_b^{(0)}+\delta_W^{(0)}) + (\delta_b^{(1)}+\delta_W^{(1)}+\delta_{\rm EW}^{(1)}+\delta_{\rm QCD}^{(1)}) \\ &+ (\delta_b^{(2)}+\delta_W^{(2)}+\delta_{\rm EW}^{(2)}+\delta_{\rm QCD}^{(2)}+\delta_{\rm EW\times QCD}^{(2)}) \\ &+ (\delta_b^{(3)}+\delta_W^{(3)}+\delta_{\rm EW}^{(3)}+\delta_{\rm QCD}^{(3)}+\delta_{\rm EW\times QCD}^{(3)})],\end{aligned} \tag{8}$$

where the LO width $\Gamma_t^{(0)} = 1.486$ GeV is obtained with $m_b = 0$ and on-shell W. The corrections from the finite b-quark mass effect and off-shell W-boson contribution are denoted by $\delta_b^{(i)}$ and $\delta_W^{(i)}$, respectively. The higher-order QCD and EW corrections are labeled as $\delta_{\rm QCD}^{(i)}$ and $\delta_{\rm EW}^{(i)}$, respectively. Adopting the SM input parameters [29]

$$\begin{aligned} &m_t = 172.69\ \text{GeV}, \quad m_b = 4.78\ \text{GeV}, \\ &m_W = 80.377\ \text{GeV}, \quad \Gamma_W = 2.085\ \text{GeV}, \\ &m_Z = 91.1876\ \text{GeV}, \quad G_F = 1.16638\times 10^{-5}\ \text{GeV}^{-2}, \end{aligned} \tag{9}$$

and choosing $|V_{tb}| = 1$ and $\alpha_s(m_Z) = 0.1179$, the N^{3}LO QCD correction is −0.667% of the LO result $\Gamma_t^{(0)}$, as shown in Table I. Adding all the other higher-order corrections that have been discussed in detail in our previous paper [16], we obtain the most accurate prediction for the top-quark width $\Gamma_t = 1.321$ GeV at $m_t = 172.69$ GeV. The scale uncertainty is reduced to ±0.2%, only half of that at NNLO. Now, the N^{3}LO and NNLO results with uncertainties are almost adjacent to each other, displaying good convergent behavior. All the formulas in the calculation are given in analytic form. The strong coupling α_s at different scales is related by an analytic solution to the three-loop renormalization group evolution equation [51,52]. As a result, our calculation is efficient and accurate. Readers can perform a customized calculation using the *Mathematica* program TopWidth [53]. In Fig. 1, we show the top-quark decay width for 170 GeV $\le m_t \le$ 175 GeV. A nearly linear dependence can be observed. For the convenience of readers, we provide a fitted function for the top-quark width within this range:

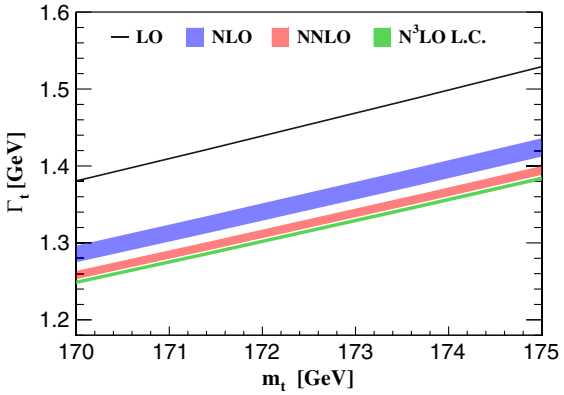

FIG. 1. Top-quark width at different values of m_t. The black line shows the LO result. The NLO, NNLO, and N^{3}LO predictions with QCD scale uncertainties are represented by the blue, red, and green bands, respectively.

$$\Gamma_t(m_t) = 0.027037 \times m_t - 3.34801\ \text{GeV}. \tag{10}$$

Our result of the top-quark decay can be applied in the calculation of the inclusive b-quark semileptonic decay $b \to X_u e\bar{\nu}_e$, which has been used to determine the CKM matrix element $|V_{ub}| = (4.19 \pm 0.17)\times 10^{-3}$ [54]. The dilepton invariant mass spectrum in the on-shell mass scheme is given by

$$\frac{{\rm d}\Gamma(b\to X_u e\bar{\nu}_e)}{{\rm d}q^2} = \Gamma_b^{(0)} \sum_{i=0} \left(\frac{\alpha_s}{\pi}\right)^i X_i\left(\frac{q^2}{m_b^2}\right), \tag{11}$$

with $\Gamma_b^{(0)} = G_F^2|V_{ub}|^2 m_b^3/96\pi^3$. An analogous expansion series in the $\overline{\rm MS}$ mass scheme can be derived using the three-loop relation between the two schemes [55]. We show such a distribution at different perturbative orders in Fig. 2. The higher-order QCD corrections significantly improve

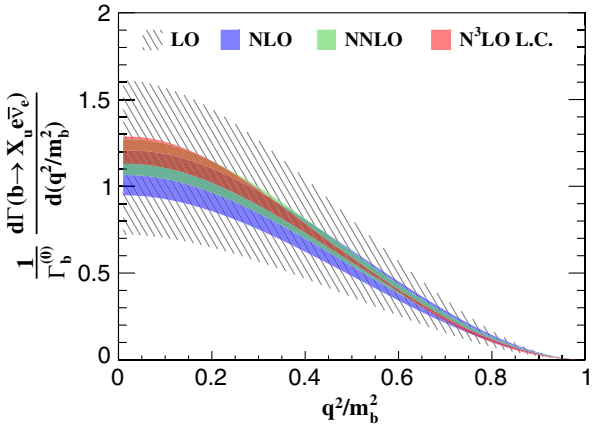

FIG. 2. The q^2/m_b^2 distribution for $b \to X_u e\bar{\nu}_e$ in the $\overline{\rm MS}$ mass scheme normalized by $\Gamma_b^{(0)}$. The bands denote the scale uncertainties.

the theoretical uncertainties caused by the variation of the renormalization scale μ by a factor of 2. For example, the scale uncertainties are around $\pm 12\%$, $\pm 9\%$, and $\pm 6\%$ at NLO, NNLO, and N^{3}LO, respectively, at $q^2/m_b^2 = 0.2$. In particular, the N^{3}LO corrections lie almost in the NNLO uncertainty band, indicating that the perturbative series converges fast in the $\overline{\text{MS}}$ mass scheme.

The inclusive b-quark semileptonic decay width can be expanded in α_s,

$$\Gamma(b \to X_u e \bar{\nu}_e) = \frac{G_F^2 |V_{ub}|^2 m_b^5}{192\pi^3}\left[1 + \sum_{i=1}\left(\frac{\alpha_s}{\pi}\right)^i b_i\right]. \quad (12)$$

The NLO and NNLO coefficients, b_1 and b_2, have been calculated in [56]. Integrating X_3 in Eq. (3) over w in the region [0, 1], we obtain the result for b_3,

$$\begin{aligned} b_3 = C_F\Bigg[& N_c^2\left(\frac{9651283}{82944} - \frac{1051339\pi^2}{62208} - \frac{67189\zeta(3)}{864} + \frac{4363\pi^4}{6480} + \frac{59\pi^2\zeta(3)}{32} + \frac{3655\zeta(5)}{96} - \frac{109\pi^6}{3780}\right) \\ & + n_l N_c\left(-\frac{729695}{27648} + \frac{48403\pi^2}{15552} + \frac{1373\zeta(3)}{108} + \frac{133\pi^4}{1728} - \frac{13\pi^2\zeta(3)}{72} - \frac{125\zeta(5)}{24}\right) + n_l^2\left(\frac{24763}{20736} - \frac{1417\pi^2}{15552} \right. \\ & \left. - \frac{37\zeta(3)}{216} - \frac{121\pi^4}{6480}\right) + \text{subleading color}\Bigg] \\ = & (-195.3 \pm 9.8) C_F. \end{aligned} \quad (13)$$

In the last line, we give a numerical estimate of the subleading color contribution, which is about 5% of the leading color result as indicated at NNLO. Our result is consistent with the estimation in [57], $b_3 = (-202 \pm 20) C_F$,

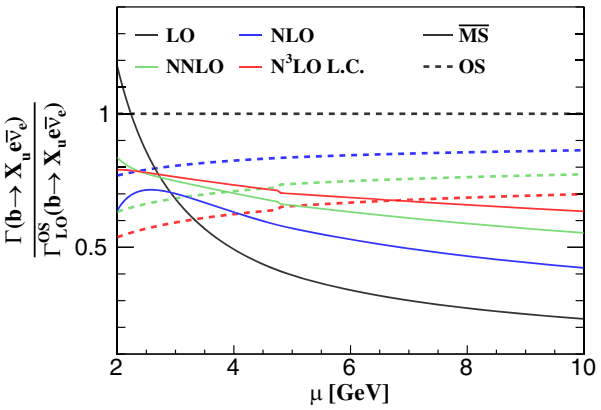

FIG. 3. Scale dependence of the b-quark semileptonic decay width normalized by the LO width in the on-shell mass scheme. The solid and dashed lines represent the results in the $\overline{\text{MS}}$ and on-shell mass schemes, respectively.

which is obtained by taking the expansion in terms of $\delta = 1 - m_u/m_b$. In Fig. 3, we show the b-quark semileptonic decay width with scale dependence in both the $\overline{\text{MS}}$ and on-shell mass schemes. The higher-order corrections are prominent in both schemes. In the on-shell mass scheme, the N^{3}LO correction decreases the NNLO result by 15%–10% when the scale varies from 2 to 10 GeV, and the scale uncertainty changes from $^{+5\%}_{-14\%}$ at NNLO to $^{+7\%}_{-17\%}$ at N^{3}LO. Such poor behavior of the perturbative series with on-shell mass is due to its sensitivity to infrared effects [58]. In contrast, the scale dependence is greatly improved in the $\overline{\text{MS}}$ scheme, changing from $\pm 20\%$ at NNLO to $\pm 11\%$ at N^{3}LO. The N^{3}LO result can be larger or less than the NNLO result depending on the scale, and the correction is about $+6\%$ at $\mu = 4.78$ GeV. The predictions in the two schemes become close to each other with more and more higher-order corrections included. Given that the current world average of the CKM matrix element V_{ub} from inclusive determination has an uncertainty of about 8% [54], smaller than or comparable to the N^{3}LO correction, the extracted value of V_{ub} in future analysis would be affected after including this N^{3}LO correction.

To summarize, we have obtained the first analytic N^{3}LO QCD leading color corrections to the top-quark decay width. This is accomplished by applying the optical theorem. The imaginary parts of four-loop integrals have been calculated with the differential equation method. All the divergences cancel out after renormalization. The final result of the decay width is vanishing if setting $m_W = m_t$ and exhibits a single logarithmic dependence on m_W when expanded around $m_W = 0$. These features serve as nontrivial checks. The N^{3}LO QCD corrections decrease the LO result by -0.667%. Combining with the other higher-order corrections, such as the EW corrections and off-shell W effects, we get the most precise theoretical prediction of the top-quark width, $\Gamma_t = 1.321$ GeV at $m_t = 172.69$ GeV, with a scale uncertainty of $\pm 0.2\%$.

Furthermore, we derive the analytic third-order QCD leading color predictions for the semileptonic $b \to u$ decay width and the dilepton invariant mass spectrum. Compared to the NNLO result, the N^{3}LO correction is about 10%–15% for different scales in the on-shell mass scheme. In the $\overline{\text{MS}}$ scheme, the N^{3}LO correction can be positive or negative depending on the scale, and the scale uncertainties are reduced significantly. The difference between the two schemes also decreases once the N^{3}LO correction is taken into account. Our reliable and accurate prediction allows for a more precise determination of the CKM matrix element V_{ub}, and it may help to resolve the long-standing discrepancy between the inclusive and exclusive determination of V_{ub} [54].

Our calculation can be extended to more differential observables, such as the invariant mass of hadronic final states or the decay into polarized W bosons. It is also

interesting to understand the simple analytic structure of four-loop integrals with massive propagators in our case. Especially, we are curious about the explanations of the symbol letters with Landau equations [59], intersection theory [60], or some other methods.

Note added. Recently, we became aware of the result by L. Chen, X. Chen, X. Guan, and Y.-Q. Ma [61], which was obtained by numerical calculation with AMFlow. We have compared the leading color results and found perfect agreement. Their results confirm that the leading color contribution accounts for 95% of the N^3LO correction, similar to the case at NNLO.

This work was supported in part by the National Natural Science Foundation of China under Grants No. 12005117, No. 12075251, No. 12175048, No. 12275156, No. 12321005, and No. 12375076. The work of L. B. C. was also supported by the Natural Science Foundation of Guangdong Province under Grant No. 2022A1515010041. The work of J. W. was also supported by the Taishan Scholar Project of Shandong Province (tsqn201909011).

[1] G. Aad *et al.* (ATLAS Collaboration), J. High Energy Phys. 06 (2023) 019.
[2] ATLAS Collaboration, Report No. ATLAS-CONF-2019-038 (2019).
[3] V. Khachatryan *et al.* (CMS Collaboration), Phys. Lett. B **736**, 33 (2014).
[4] F. Caola and K. Melnikov, Phys. Rev. D **88**, 054024 (2013).
[5] P. P. Giardino and C. Zhang, Phys. Rev. D **96**, 011901 (2017).
[6] A. Baskakov, E. Boos, and L. Dudko, Phys. Rev. D **98**, 116011 (2018).
[7] C. Herwig, T. Ježo, and B. Nachman, Phys. Rev. Lett. **122**, 231803 (2019).
[8] T. Horiguchi, A. Ishikawa, T. Suehara, K. Fujii, Y. Sumino, Y. Kiyo, and H. Yamamoto, arXiv:1310.0563.
[9] Z. Li, X. Sun, Y. Fang, G. Li, S. Xin, S. Wang, Y. Wang, Y. Zhang, H. Zhang, and Z. Liang, Eur. Phys. J. C **83**, 269 (2023); **83**, 501(E) (2023).
[10] H. Abramowicz *et al.* (CLICdp Collaboration), J. High Energy Phys. 11 (2019) 003.
[11] M. Jezabek and J. H. Kuhn, Nucl. Phys. **B314**, 1 (1989).
[12] A. Czarnecki, Phys. Lett. B **252**, 467 (1990).
[13] C. S. Li, R. J. Oakes, and T. C. Yuan, Phys. Rev. D **43**, 3759 (1991).
[14] J. Gao, C. S. Li, and H. X. Zhu, Phys. Rev. Lett. **110**, 042001 (2013).
[15] M. Brucherseifer, F. Caola, and K. Melnikov, J. High Energy Phys. 04 (2013) 059.
[16] L.-B. Chen, H. T. Li, J. Wang, and Y. Wang, Phys. Rev. D **108**, 054003 (2023).
[17] A. Czarnecki and K. Melnikov, Nucl. Phys. **B544**, 520 (1999).
[18] K. G. Chetyrkin, R. Harlander, T. Seidensticker, and M. Steinhauser, Phys. Rev. D **60**, 114015 (1999).
[19] I. R. Blokland, A. Czarnecki, M. Slusarczyk, and F. Tkachov, Phys. Rev. Lett. **93**, 062001 (2004).
[20] I. R. Blokland, A. Czarnecki, M. Slusarczyk, and F. Tkachov, Phys. Rev. D **71**, 054004 (2005); **79**, 019901 (E) (2009).
[21] A. Czarnecki and K. Melnikov, Phys. Rev. Lett. **88**, 131801 (2002).
[22] A. Czarnecki, J. G. Korner, and J. H. Piclum, Phys. Rev. D **81**, 111503 (2010).
[23] A. Czarnecki, S. Groote, J. G. Körner, and J. H. Piclum, Phys. Rev. D **97**, 094008 (2018).
[24] R.-Q. Meng, S.-Q. Wang, T. Sun, C.-Q. Luo, J.-M. Shen, and X.-G. Wu, Eur. Phys. J. C **83**, 59 (2023).
[25] L.-B. Chen and J. Wang, Phys. Lett. B **786**, 453 (2018).
[26] S. Datta, N. Rana, V. Ravindran, and R. Sarkar, arXiv:2308.12169.
[27] A. Denner and T. Sack, Nucl. Phys. **B358**, 46 (1991).
[28] G. Eilam, R. R. Mendel, R. Migneron, and A. Soni, Phys. Rev. Lett. **66**, 3105 (1991).
[29] R. L. Workman *et al.* (Particle Data Group), Prog. Theor. Exp. Phys. **2022**, 083C01 (2022).
[30] Q.-f. Wu and Z. Li, arXiv:2310.07634.
[31] P. Nogueira, J. Comput. Phys. **105**, 279 (1993).
[32] J. Kuipers, T. Ueda, J. A. M. Vermaseren, and J. Vollinga, Comput. Phys. Commun. **184**, 1453 (2013).
[33] V. Shtabovenko, R. Mertig, and F. Orellana, Comput. Phys. Commun. **256**, 107478 (2020).
[34] A. V. Smirnov and F. S. Chuharev, Comput. Phys. Commun. **247**, 106877 (2020).
[35] S. Laporta, Int. J. Mod. Phys. A **15**, 5087 (2000).
[36] F. V. Tkachov, Phys. Lett. **100B**, 65 (1981).
[37] K. G. Chetyrkin and F. V. Tkachov, Nucl. Phys. **B192**, 159 (1981).
[38] A. V. Kotikov, Phys. Lett. B **254**, 158 (1991).
[39] A. V. Kotikov, Phys. Lett. B **267**, 123 (1991); **295**, 409(E) (1992).
[40] J. M. Henn, Phys. Rev. Lett. **110**, 251601 (2013).
[41] R. N. Lee, Comput. Phys. Commun. **267**, 108058 (2021).
[42] E. Remiddi and J. A. M. Vermaseren, Int. J. Mod. Phys. A **15**, 725 (2000).
[43] D. Maitre, Comput. Phys. Commun. **174**, 222 (2006).
[44] X. Liu, Y.-Q. Ma, and C.-Y. Wang, Phys. Lett. B **779**, 353 (2018).
[45] X. Liu and Y.-Q. Ma, Comput. Phys. Commun. **283**, 108565 (2023).
[46] H. Ferguson and D. Bailey (1992), A polynomial time, numerically stable integer relation algorithm, Report No. RNR-91-032, NASA Ames Research Center.

[47] H. Ferguson, D. Beiley, and S. Arno, Math. Comput. **68**, 351 (1999).
[48] See Supplemental Material at http://link.aps.org/supplemental/10.1103/PhysRevD.109.L071503 for the complete analytical results of the leading color N^3LO QCD corrections.
[49] M. Bohm, H. Spiesberger, and W. Hollik, Fortschr. Phys. **34**, 687 (1986).
[50] A. Denner and T. Sack, Z. Phys. C **46**, 653 (1990).
[51] E. Gardi, G. Grunberg, and M. Karliner, J. High Energy Phys. 07 (1998) 007.
[52] A. Deur, S. J. Brodsky, and G. F. de Teramond, Nucl. Phys. **90**, 1 (2016).
[53] The program can be downloaded from https://github.com/haitaoli1/TopWidth or the Supplemental Material.
[54] Y. S. Amhis *et al.* (HFLAV Collaboration), Phys. Rev. D **107**, 052008 (2023).
[55] K. Melnikov and T. van Ritbergen, Phys. Lett. B **482**, 99 (2000).
[56] T. van Ritbergen, Phys. Lett. B **454**, 353 (1999).
[57] M. Fael, K. Schönwald, and M. Steinhauser, Phys. Rev. D **104**, 016003 (2021).
[58] M. Beneke and V. M. Braun, Nucl. Phys. **B426**, 301 (1994).
[59] C. Dlapa, M. Helmer, G. Papathanasiou, and F. Tellander, J. High Energy Phys. 10 (2023) 161.
[60] J. Chen, B. Feng, and L. L. Yang, Sci. China Phys. Mech. Astron. **67**, 221011 (2024).
[61] L. Chen, X. Chen, X. Guan, and Y.-Q. Ma, arXiv:2309.01937.